

## 纺锤形 $\beta$ -FeOOH 纳米结构和 $\alpha$ -氧化铁亚微米/微米粒子的合成与转变

郭培志<sup>\*,1</sup> 谭金山<sup>1</sup> 季倩倩<sup>1</sup> 赵 丹<sup>1</sup> 赵修松<sup>1,2</sup>

(<sup>1</sup> 青岛大学纤维新材料与现代纺织国家重点实验室培育基地, 化学化工与环境学院, 青岛 266071)

(<sup>2</sup>Department of Chemical and Biomolecular Engineering, National University of Singapore,  
4 Engineering Drive 4, Singapore 117576 Singapore)

**摘要:** 使用一种简易的无表面活性剂辅助的水热合成方法, 在温度为 140 °C 时实现了纺锤形  $\beta$ -FeOOH 纳米结构向  $\alpha$ -氧化铁亚微米/微米粒子的转变。研究表明, 通过实验参数的简单调控, 实现了单晶  $\alpha$ -氧化铁亚微米粒子与  $\beta$ -FeOOH 的纺锤形纳米结构和纳米棒的控制制备。基于实验结果, 提出了该过程中的相转变机理。

**关键词:**  $\alpha$ -氧化铁;  $\beta$ -FeOOH; 水热合成; 相转变

中图分类号: O614.8; O611.62

文献标识码: A

文章编号: 1001-4861(2009)04-0647-05

## $\beta$ -FeOOH Nanospindles: Facile Synthesis and Their Transition to $\alpha$ -Fe<sub>2</sub>O<sub>3</sub> Submicron/Micro-particles

GUO Pei-Zhi<sup>\*,1</sup> TAN Jin-Shan<sup>1</sup> JI Qian-Qian<sup>1</sup> ZHAO Dan<sup>1</sup> ZHAO Xiu-Song<sup>1,2</sup>

(<sup>1</sup>Laboratory of New Fiber Materials and Modern Textile, The Growing Base for State Key Laboratory, School of Chemistry,  
Chemical Engineering and Environmental Sciences, Qingdao University, Qingdao, Shandong 266071)

(<sup>2</sup>Department of Chemical and Biomolecular Engineering, National University of Singapore,  
4 Engineering Drive 4, Singapore 117576 Singapore)

**Abstract:** The transition of akaganeite( $\beta$ -FeOOH) nanospindles to hematite( $\alpha$ -Fe<sub>2</sub>O<sub>3</sub>) submicron/micro-particles has been studied through a facile surfactant-free hydrothermal method at 140 °C. Single crystal  $\alpha$ -Fe<sub>2</sub>O<sub>3</sub> submicron particles and  $\beta$ -FeOOH nanospindles or nanorods can be controllably fabricated by simply changing the experimental parameters. The mechanism of the phase transition is proposed based on the experimental results.

**Key words:**  $\alpha$ -Fe<sub>2</sub>O<sub>3</sub>;  $\beta$ -FeOOH; hydrothermal synthesis; phase transition

The physical and chemical properties of nanostructured materials from transition metals and their oxide are essentially different from those of bulk materials and largely dependent on their size, shape and surface chemistry<sup>[1,2]</sup>. The synthesis of such nanomaterials is also important in nanotechnology research due to their potential and practical applications<sup>[3,4]</sup>. Among the materi-

als, Fe<sub>2</sub>O<sub>3</sub> is very attractive due to its nontoxicity, low cost, good stability and wide applications in gas sensors<sup>[5,6]</sup>, catalysis<sup>[7-9]</sup>, magnetic recording materials and lithium-ion batteries<sup>[10,11]</sup>.

Many Fe<sub>2</sub>O<sub>3</sub> nanostructures with various morphologies have been fabricated by different methods<sup>[12-22]</sup>. For example, forced hydrolysis of homogenous solutions of

收稿日期: 2008-11-14. 收修改稿日期: 2009-01-31.

国家自然科学基金(No.20803037), 山东省博士基金(No.2007BS04022)和胶体与界面化学教育部重点实验室(山东大学)开放课题资助项目。

\*通讯联系人。E-mail: pzguo@qdu.edu.cn

第一作者: 郭培志, 男, 31 岁, 副教授; 研究方向: 微纳材料结构与性能。

ferric ions developed mainly by Matijevic and his co-workers has been used to synthesis hematite nanoparticles<sup>[12,13]</sup>.  $\text{Fe}_2\text{O}_3$  nanobelts and nanowires could be synthesized by direct thermal oxidation of Fe substrates<sup>[14]</sup> and  $\text{Fe}_2\text{O}_3$  nanorings were synthesized by a microwave-assisted hydrothermal process from the aqueous systems of  $\text{FeCl}_3$  and  $\text{NH}_4\text{H}_2\text{PO}_4$ <sup>[15]</sup>. Airplane-like  $\text{FeOOH}$ ,  $\text{Fe}_2\text{O}_3$  nanostructures,  $\alpha\text{-FeOOH}$  and  $\alpha\text{-Fe}_2\text{O}_3$  nanorods were obtained via the hydrothermal processes<sup>[16,17]</sup>.

Generally,  $\text{FeOOH}$  nanostructures could be synthesized by regulating the pH value of initial systems and their transition to  $\text{Fe}_2\text{O}_3$  nanostructures could be obtained by adjusting the processing temperature in air or longtime aging<sup>[13,16~18]</sup>. However, it still remains unclear about the phase transition from  $\text{FeOOH}$  to  $\text{Fe}_2\text{O}_3$  under hydrothermal conditions.

In this work, the transition of akaganeite ( $\beta\text{-FeOOH}$ ) nanospindles to hematite ( $\alpha\text{-Fe}_2\text{O}_3$ ) submicron/micro-particles has been realized at 140 °C through a simple surfactant-free hydrothermal method by changing the synthesis time. Furthermore,  $\beta\text{-FeOOH}$  nanospindles and nanorods can be fabricated at a lower temperature, while uniform  $\alpha\text{-Fe}_2\text{O}_3$  submicron/micro-particles are obtained at a higher temperature.

## 1 Experimental

Alcohols (A.R.) and  $\text{FeCl}_3$  (A.R.) were purchased from Sinopharm Chemical Reagent Company and used without further purification. In a typical synthesis,  $\text{FeCl}_3$  (0.487 g) was dissolved in distilled water (30 mL) under stirring. And then the mixture was transferred to a 40 mL teflon lined autoclave. Hydrothermal synthesis was carried out in an oven at 140 °C for 2~24 h. The products were collected by filtration, washed with distilled water and ethanol for several times each, and then dried in an oven at 60 °C for 6 h.

X-ray powder diffraction (XRD) measurements were performed using a Bruker D8 advanced X-ray diffractometer equipped with graphite monochromatized  $\text{Cu K}\alpha$  radiation ( $\lambda = 0.15418$  nm) from 10° to 80° ( $2\theta$ ) and operated at 40 kV and 40 mA using a one-dimensional detector. Scanning electron microscopy (SEM) images were taken with a JSM-6390LV scanning electron mi-

croscope operated at 20 kV. Transmission electron microscopy (TEM) and high resolution transmission electron microscopy (HRTEM) images were obtained with a JEM-2000EX and JEM-2100 transmission electron microscope operated at 160 kV and 200 kV, respectively.

## 2 Results and discussion

XRD patterns of the as-synthesized products are shown in Fig.1. The diffraction peaks of the precipitate in Fig.1A can be clearly indexed to tetragonal akaganeite phase ( $\beta\text{-FeOOH}$ , PDF 75-1594) and no obvious impurity can be observed in the samples synthesized at 110 °C even though the synthesis time is 24 h.

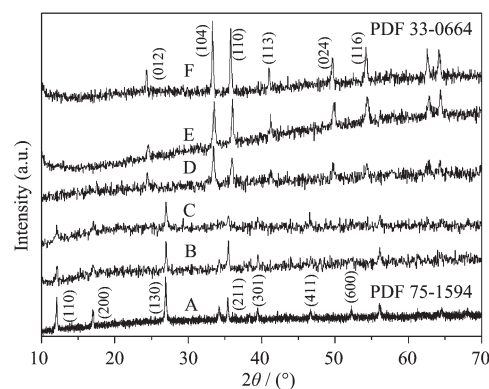


Fig.1 XRD patterns of the products synthesized at 110 °C for 24 h (A), at 140 °C for 2 h (B), 3 h (C), 6 h (D) and 24 h (E), and at 170 °C for 3 h (F)

When the synthesis temperature is increased to 140 °C, the tetragonal akaganeite phase can also be seen from the XRD pattern of the sample when the synthesis time is 2 h, as shown in Fig.1B. The main peaks of the akaganeite phase are still obtained with the synthesis time up to 3 h (Fig.1C), however, the peak with a  $2\theta$  value of 35.40°, which can be ascribed to (211) peak of the akaganeite phase, are weakened and a new peak with a  $2\theta$  value of 35.80° appears, which can be ascribed to (110) peak of the hematite phase. If the synthesis time is prolonged to 6 h (Fig.1D), pure hematite phase ( $\alpha\text{-Fe}_2\text{O}_3$ , PDF 33-0664) can be formed. And the hematite phase is not changed with the synthesis time up to 24 h (Fig.1E). When the temperature is further increased to 170 °C, the hematite phase can be observed from the XRD pattern (Fig.1F) of the products with the

synthesis time of 3 h, which is in accord with previous reports<sup>[13]</sup>.

The morphology of the samples was examined with scanning electron microscope. As shown in Fig. 2A and B, nanospindles and nanorods with the aspect ratios of 5~12 for the  $\beta$ -FeOOH phase are observed when the synthesis temperature is 110 °C and the synthesis times are 3 h and 24 h, respectively. If the

temperature is 170 °C, relatively uniform  $\alpha$ -Fe<sub>2</sub>O<sub>3</sub> sub-micron particles with the diameters of 90~130 nm are dispersed with the synthesis time of 3 h, while polyhedral  $\alpha$ -Fe<sub>2</sub>O<sub>3</sub> submicron particles with the diameters of 150~250 nm are obtained when the synthesis time is elongated to 6 h. Further prolonging the synthesis time to 24 h, the diameters of the  $\alpha$ -Fe<sub>2</sub>O<sub>3</sub> particles are almost unchanged.

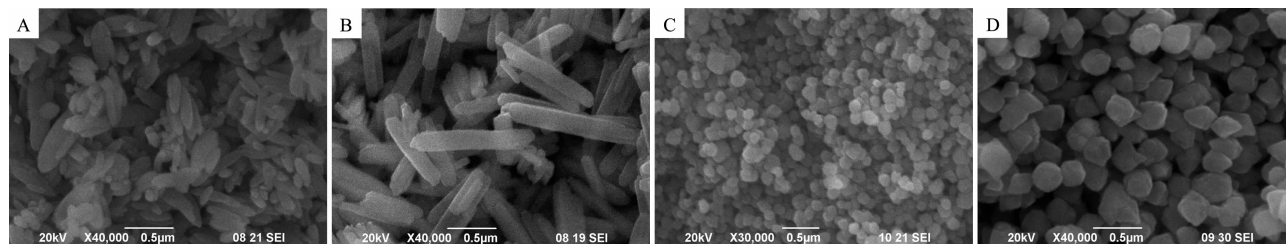


Fig.2 SEM images of the products synthesized at 110 °C for 3 h (A) and 2 h (B); and at 170 °C for 3 h (C) or 6 h (D)

It is interesting to note that the morphologies of the samples change greatly concomitant with the phase transition when the synthesis temperature is 140 °C, as shown in Fig.3.  $\beta$ -FeOOH Nanospindles are obtained when the synthesis time is 2 h (Fig.3A) and a small quantity of  $\alpha$ -Fe<sub>2</sub>O<sub>3</sub> particles can be formed with the time of 3 h (Fig.3B). Clearly, only uniform  $\alpha$ -Fe<sub>2</sub>O<sub>3</sub> sub-

micron particles with the size of about 70~100 nm can be observed for the time of 6 h (Fig.3C). Finally,  $\alpha$ -Fe<sub>2</sub>O<sub>3</sub> microparticles with the side length of 1.5~2.5 µm with octahedral or truncated cubic morphologies are obtained when the synthesis time is 24 h (Fig.3D and the inset). Further increasing the synthesis time to 72 h, the micro-scale  $\alpha$ -Fe<sub>2</sub>O<sub>3</sub> particles contracted somewhat.

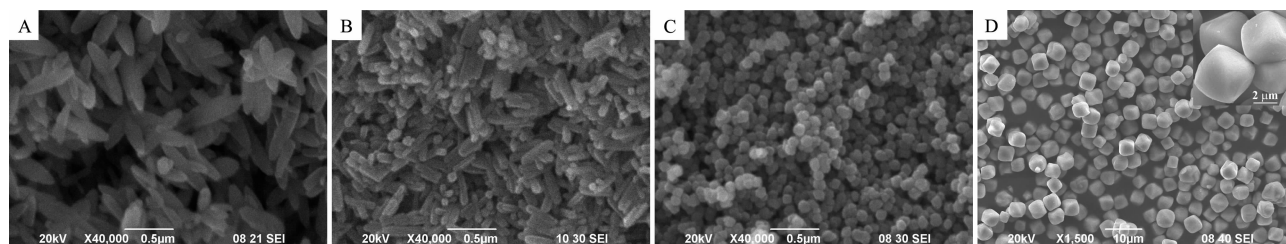


Fig.3 SEM images of the products synthesized from aqueous ferric solutions at 140 °C for 2 h (A), 3 h (B), 6 h (C) and 24 h (D)

The micro/nano-structures of the samples were further examined with transmission electron microscope. As shown in Fig.4, the spindle-like structure of  $\beta$ -FeOOH (Fig.4A) and some ripplelike contrast can be observed and the ED patterns of one spindle denote that the  $\beta$ -FeOOH nanospindles are well crystallized, as shown in the inset in Fig.4A. It is seen from the HRTEM image of a  $\beta$ -FeOOH nanospindle (Fig.4B) that the fringe spacing of 0.22 nm concurs well with the interplanar spacing of the plane (301) and some defects are also found, indicating that the nanospindles are formed with a preferred growth direction of [301]. It can

be seen that  $\alpha$ -Fe<sub>2</sub>O<sub>3</sub> submicron particles are relatively uniform and the ED patterns of one particle (the inset in Fig.4C) show the single-crystal nature of  $\alpha$ -Fe<sub>2</sub>O<sub>3</sub> sub-micron particles. The HRTEM images of the particle (Fig.4D) further confirm the formation of the single-crystal structures. The fringes are separated by 0.27 nm, which agrees well with the (104) lattice spacing of the rhombohedral hematite.

With the difference from those results of Fe(OH)<sub>3</sub> gel systems<sup>[13]</sup>, in this work, the  $\beta$ -FeOOH nanospindles are obtained at the beginning of the reaction when the synthesis temperature is 110 °C. It appears that aka-

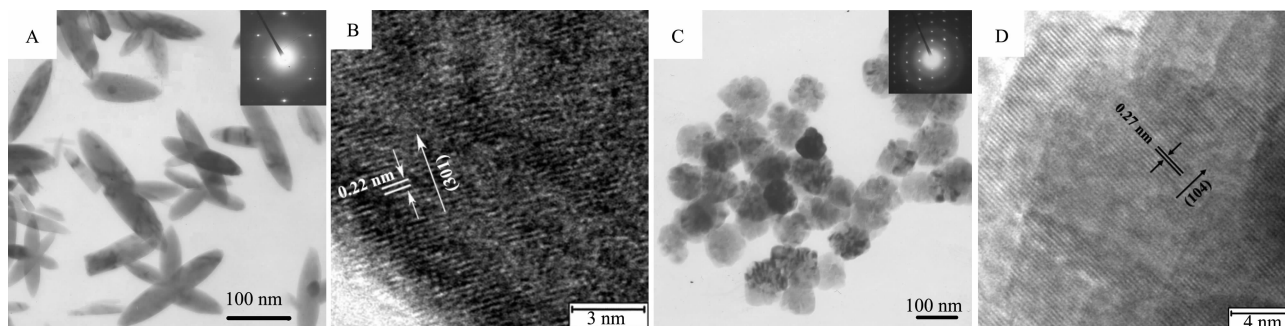
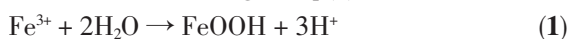
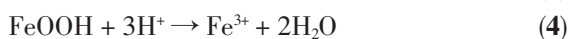
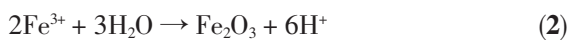


Fig.4 TEM and HRTEM images of  $\beta$ -FeOOH nanospindles (A, B) and  $\alpha$ -Fe<sub>2</sub>O<sub>3</sub> nanoparticles (C, D).  
Samples as used in Fig.3A and 3C

ganeite is formed according to Eq (1),



$\beta$ -FeOOH nanorods are obtained with the synthesis time elongated to 24 h, indicating that the akaganeite phase can not be transferred to the hematite phase under such conditions. When the synthesis temperature is increased to 140 °C, Eq(1) occurs first based on the SEM and TEM results. These results are contradictory with those predications that the Eq (2) occurs from the beginning under those conditions<sup>[12]</sup>. If the FeOOH nanostructures are heated in air, Eq(3) could occur and the morphology of the samples is almost unchanged<sup>[16,17]</sup>. However, our detailed experimental results show that the formation of  $\alpha$ -Fe<sub>2</sub>O<sub>3</sub> submicron particles are gradually formed by the dissolution of  $\beta$ -FeOOH nanospindles under hydrothermal conditions, as shown in Eq(4) and Eq (2). The single crystal nature of the  $\alpha$ -Fe<sub>2</sub>O<sub>3</sub> submicron particles can be observed from the corresponding ED patterns and HRTEM images. It should be noted that the transition time from the akaganeite phase to the hematite phase under such hydrothermal processes is much shorter than that of ferric hydroxide gel systems<sup>[13]</sup>. With the elongation of the synthesis time, micro-scale  $\alpha$ -Fe<sub>2</sub>O<sub>3</sub> particles with special geometries can be gradually obtained.



When further increasing the synthesis temperature to 170 °C, Eq(2) appears first and  $\alpha$ -Fe<sub>2</sub>O<sub>3</sub> submicron particles with narrow size distributions are obtained by changing the synthesis time. Interestingly, the size of the submicron particles are almost unchanged for the

synthesis time of 6~24 h, indicating that the formation dynamics of the particles is temperature-dependent only. Magnetic properties of  $\alpha$ -Fe<sub>2</sub>O<sub>3</sub> submicron particles and template effect on  $\alpha$ -Fe<sub>2</sub>O<sub>3</sub> submicron particles formation are currently under study.

### 3 Conclusions

Single crystal  $\alpha$ -Fe<sub>2</sub>O<sub>3</sub> submicron particles with relatively uniform size are synthesized through a simple hydrothermal method and the transition of the  $\beta$ -FeOOH nanospindles to  $\alpha$ -Fe<sub>2</sub>O<sub>3</sub> submicron particles has been realized at 140 °C by changing the synthesis time. Spindle-/rod-like nanostructures of the  $\beta$ -FeOOH phase as well as submicron/micro-particles of the  $\alpha$ -Fe<sub>2</sub>O<sub>3</sub> phase can be easily fabricated by controlling the experimental parameters.

### References:

- [1] Burda C, Chen X B, Narayanan R, et al. *Chem. Rev.*, **2005**, *105*:1025~1102
- [2] Bratlie K M, Lee H, Komvopoulos K, et al. *Nano Lett.*, **2007**, *7*:3097~3101
- [3] Kim D, Park J, An K, et al. *J. Am. Chem. Soc.*, **2007**, *129*: 5812~5813
- [4] Lee H, Habas S E, Somorjai G A, et al. *J. Am. Chem. Soc.*, **2008**, *130*:5406~5407
- [5] Fukazawa M, Matuzaki H, Hara K. *Sens. Actuators B*, **1993**, *14*:521~522
- [6] Huo L H, Li Q, Zhao H, et al. *Sens. Actuators B*, **2005**, *107*: 915~920
- [7] Frank S N, Bard A J. *J. Phys. Chem.*, **1977**, *81*:1484~1488
- [8] Ohmori T, Takahashi H, Mametsuka H, et al. *Phys. Chem. Chem. Phys.*, **2000**, *2*:3519~3522

- [9] Cesar I, Kay A, Gonzalez-Martinez J A, et al. *J. Am. Chem. Soc.*, **2006**,**128**:4582~4583
- [10] Poizot P, Laruelle S, Grugeon S, et al. *Nature*, **2000**,**407**:496~499
- [11] Wu C, Yin P, Zhu X, et al. *J. Phys. Chem. B*, **2006**,**110**:17806~17812.
- [12] Hamada S, Matijevic E. *J. Chem. Soc., Faraday Trans. I*, **1982**, **78**:2147~2156
- [13] Riveros P A, Dutrizac J E. *Hydrometallurgy*, **1997**,**46**:85~104
- [14] Wen X G, Wang S H, Ding Y, et al. *J. Phys. Chem. B*, **2005**, **109**:215~220
- [15] Hu X L, Yu J C, Gong J M, et al. *Adv. Mater.*, **2007**,**19**:2324~2329
- [16] Li S Z, Zhang H, Wu J B. *Cryst. Growth Des.*, **2006**,**6**:351~353
- [17] Tang B, Wang G L, Zhuo L H. *Inorg. Chem.*, **2006**,**45**:5196~5200
- [18] Music S, Krehula S, Popovic S. *Mater. Lett.*, **2004**,**58**:444~448
- [19] Wang W, Howe J Y, Gu B H. *J. Phys. Chem. C*, **2008**,**112**:9203~9208
- [20] Wang G X, Gou X L, Horvat J, et al. *J. Phys. Chem. C*, **2008**, **112**:15220~15225
- [21] Fu Y Y, Chen J, Zhang H. *Chem. Phys. Lett.*, **2001**,**350**:491~494
- [22] Salazar-Alvarez G, Qin J, Sepelak, et al. *J. Am. Chem. Soc.*, **2008**,**130**:13234~13239